

Stern- und
Planetenentstehung
Sommersemester 2020
Markus Röllig

Lecture 2: Observing Young Stars



http://exp-astro.physik.uni-frankfurt.de/star_formation/index.php

VORLESUNG/LECTURE

Raum: Physik - 02.201a

dienstags, 12:00 - 14:00 Uhr

SPRECHSTUNDE:

Raum: GSC, 1/34, Tel.: 47433, (roellig@ph1.uni-koeln.de)

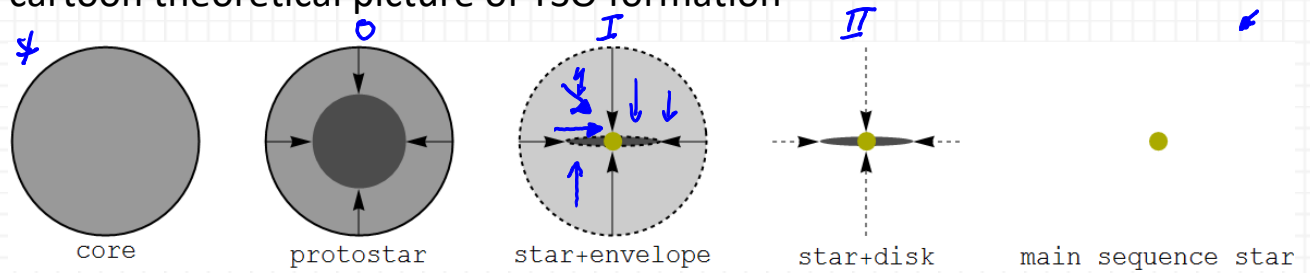
dienstags: 14:00-16:00 Uhr

Nr.	Thema	Termin
1	Observing the cold ISM	21.04.2020
2	Observing Young Stars	28.04.2020
3	Gas Flows and Turbulence Magnetic Fields and Magnetized Turbulence	05.05.2020
4	Gravitational Instability and Collapse	12.05.2020
5	Stellar Feedback	19.05.2020
6	Giant Molecular Clouds	26.05.2020
7	Star Formation Rate at Galactic Scales	02.06.2020
8	Stellar Clustering	09.06.2020
9	Initial Mass Function – Observations and Theory	16.06.2020
10	Massive Star Formation	23.06.2020
11	Protostellar disks and outflows – observations and theory	30.06.2020
12	Protostar Formation and Evolution	07.07.2020
13	Late Stage stars and disks – planet formation	14.07.2020

2 OBSERVING YOUNG STARS

2.1 CLASSIFICATION AND EVOLUTION OF YOUNG STARS

cartoon theoretical picture of YSO formation



- core: warm gas & dust
- proto-star: hot condensation, cooler envelope, accretion reduces opacity
- star + envelope NIR transparent envelope, star directly visible
- star + disk: envelope completely accreted onto disk + star
- m.s. star star contracts onto MS (main sequence)

What would these stages look like?

2.1.1 Class 0 sources

How can we detect a collapsing core?

SED

SPECTRAL ENERGY DISTRIBUTION -- SED

SEDs are energy plotted against some measure of the photon -- frequency or wavelength.

The units that are used in Spitzer data are Janskys. $1 \text{ Jy} = 10^{-23} \text{ erg/s/cm}^2/\text{Hz}$ (in cgs units rather than mks units, sorry -- and just to be clear, I mean $\text{erg} / (\text{s} \cdot \text{cm}^2 \cdot \text{Hz})$, it's just easier to read in the way I wrote it above). A Jansky is technically a unit of "flux density," represented by F_ν .

We want to plot "energy density". One way to do is to get rid of the "per Hz", e.g., multiply the Jy by the frequency (ν) of the bandpass center, or νF_ν .

$F_\nu \cdot d\nu = F_\lambda d\lambda$

$$\frac{dF}{d\lambda} = \frac{dF}{d\nu} \frac{d\nu}{d\lambda} \quad \text{and} \quad d\nu = \frac{c}{\lambda^2} d\lambda$$

$$\lambda F_\lambda = \lambda \frac{c}{\lambda^2} F_\nu$$

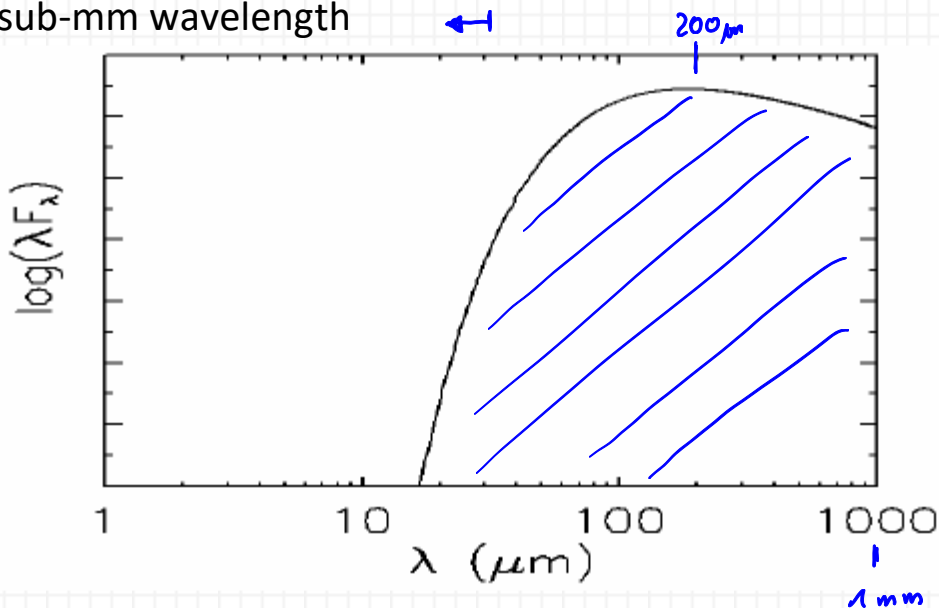
$c = \lambda \cdot \nu \quad \nu = \frac{c}{\lambda}$

$$B_\lambda = \frac{2 h \frac{c^2}{\lambda^5}}{\exp\left(\frac{h c}{\lambda k T}\right) - 1} \quad \text{and} \quad \lambda B_\lambda = \frac{2 h \frac{c^2}{\lambda^4}}{\exp\left(\frac{h c}{\lambda k T}\right) - 1}$$

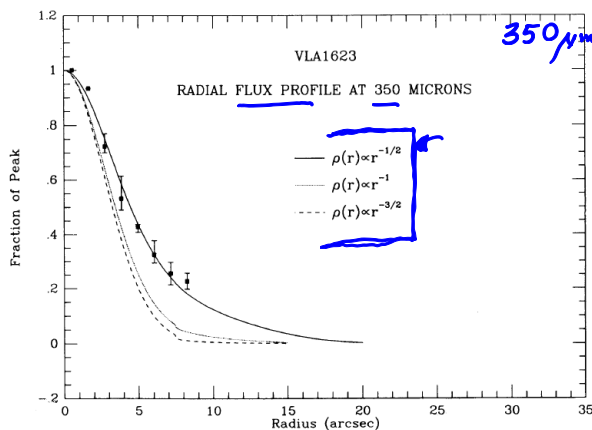
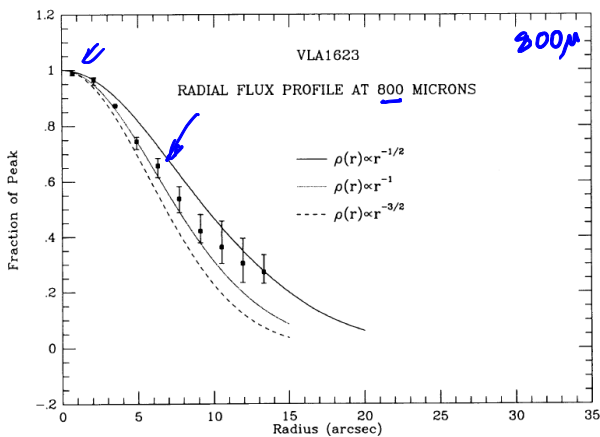
- thermal emission of the warm condensation

- compact (few 1000 AU)
- sub-mm wavelength

$1 \text{ AU} \approx 150 \cdot 10^6 \text{ km}$



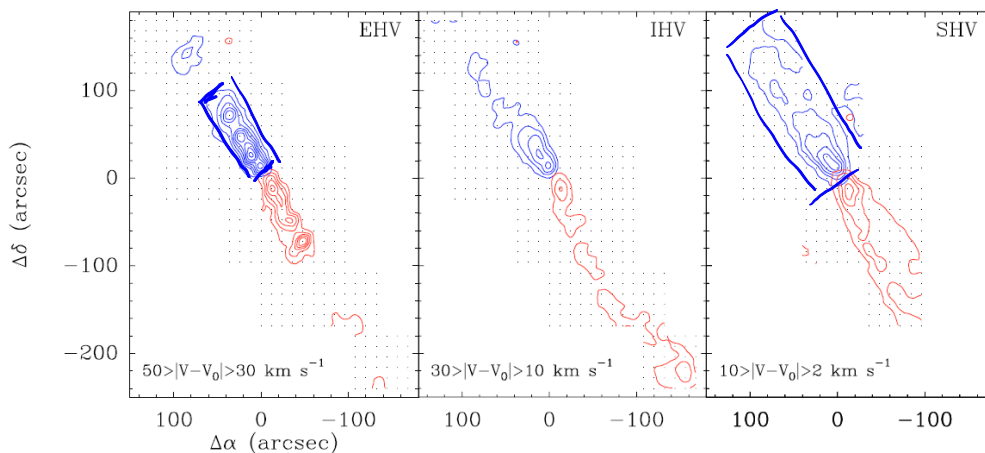
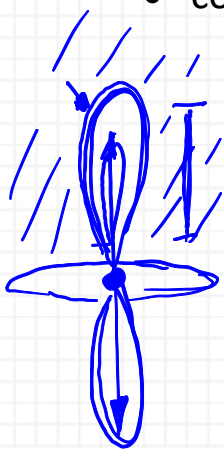
- interferometric observations



Flux vs. radius at 800 and 350μm for source VLA1623 (Andre et al. 1993). At the distance of the source, $1'' = 130 \text{ AU}$

- collapse produces outflows -> outflow signatures

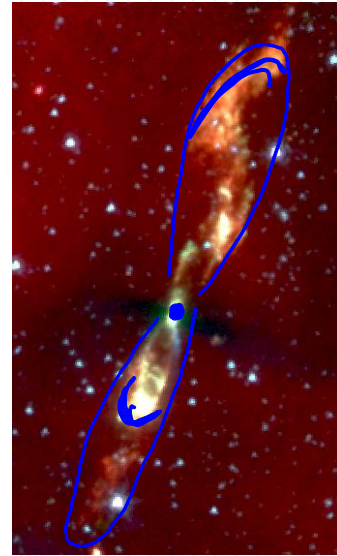
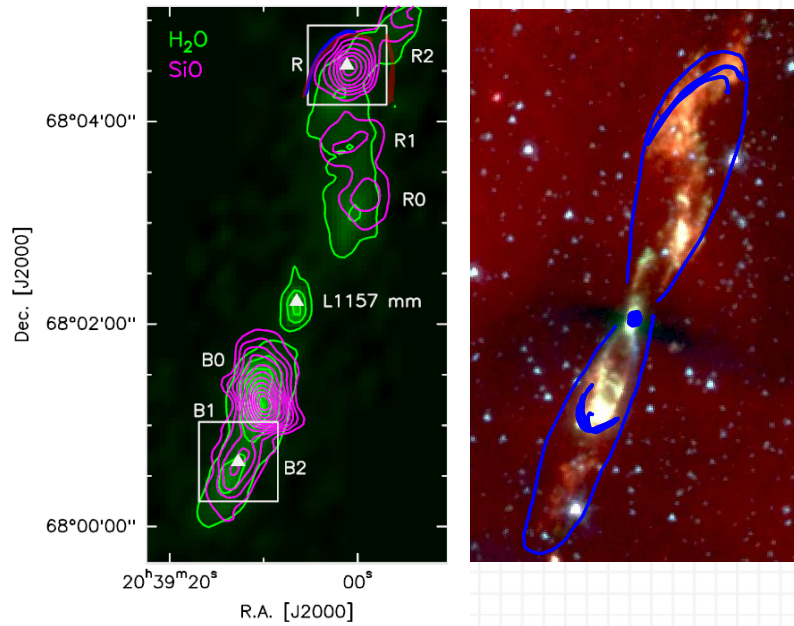
- high velocities in molecular lines (bi-polar)



CO (2-1) contours (spaced 1 km/s) in Taurus (Tafalla et al. 2004)



- indirect: high E excited molecular line emission (shocks)
e.g. $\text{SiO } J=2-1$ (Santangelo et al. 2013 & Spitzer IRAC
NASA/JPL-Caltech/UIUC & Caltech/SSC)



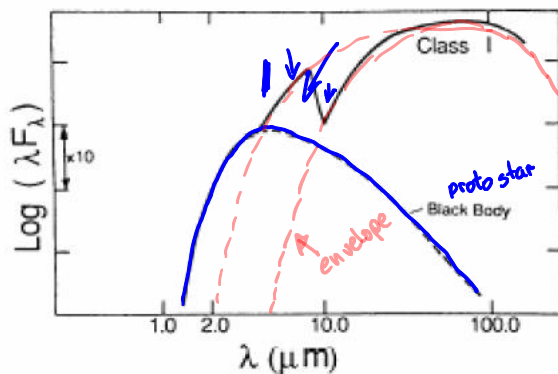
- SiO produced in warm shocks (grain sputtering?)
- Regions with one of these signs \rightarrow Class 0 sources

2.1.2 Class 1 sources

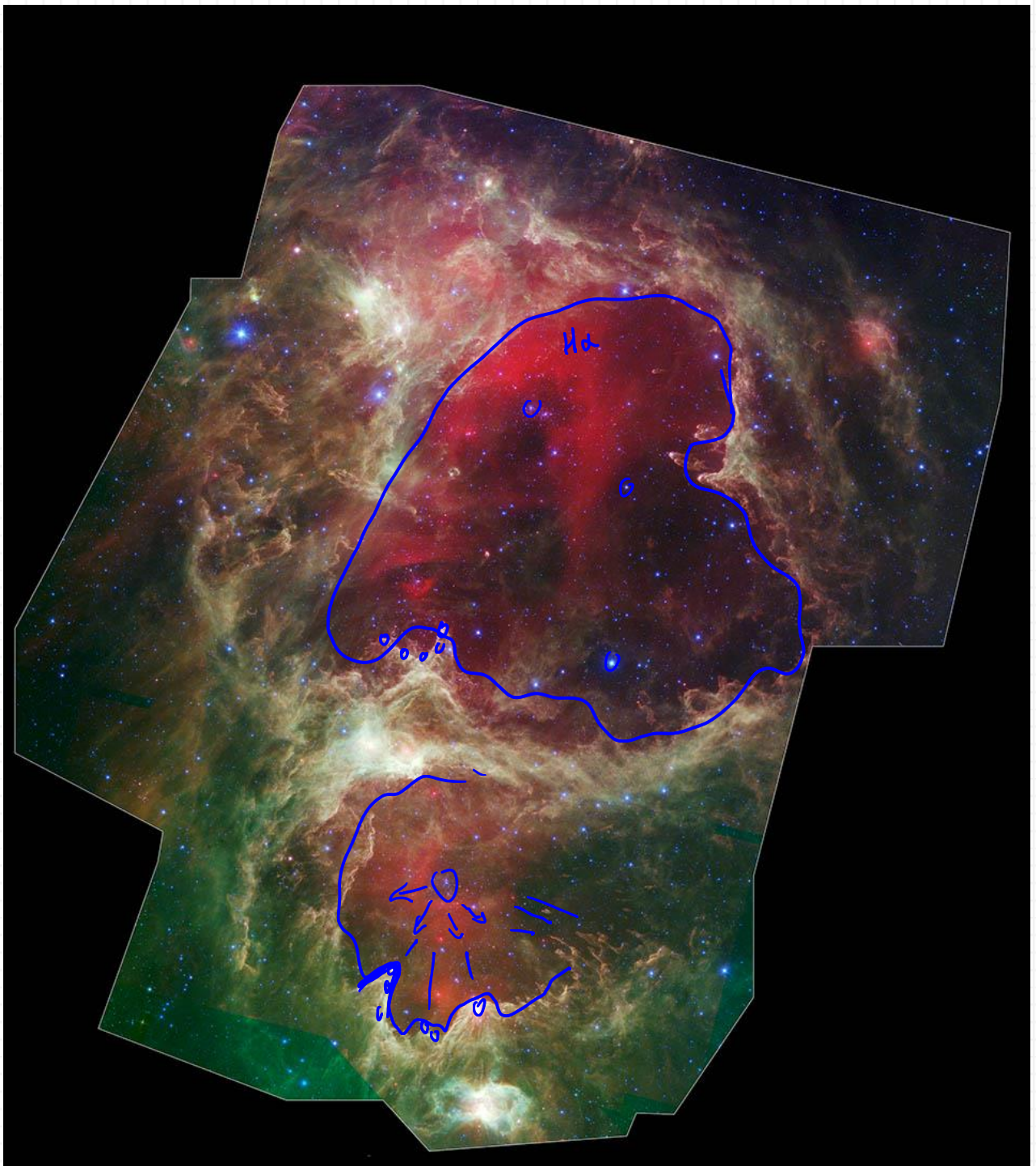
distinction from class 0 \rightarrow protostar detected in IR

SED is broader than single-T BB function and shows MIR & NIR excess
(Excess IR comes from large amounts of circum-protostellar dust)

10 μm silicate absorption feature clearly present



$\sim 1/3$ of all gas cores identified by thermal dust or molecular line emission show evidence for an IR source at the center – best seen in distant regions of massive star formation \rightarrow clusters



W5: Mountains of creation - NASA/JPL-Caltech/L. Allen & X. Koenig (Harvard-Smithsonian CfA)
dark blue: 3.6 μm ,light blue:4.5 μm , green: 8.0 μm , red: 24.0 μm

In nearby regions the resolution is enough to see individual sources inside a core.

In some source the contours of mm (cold) and IR (hot) emission correspond to each other \rightarrow something is heating up the center.

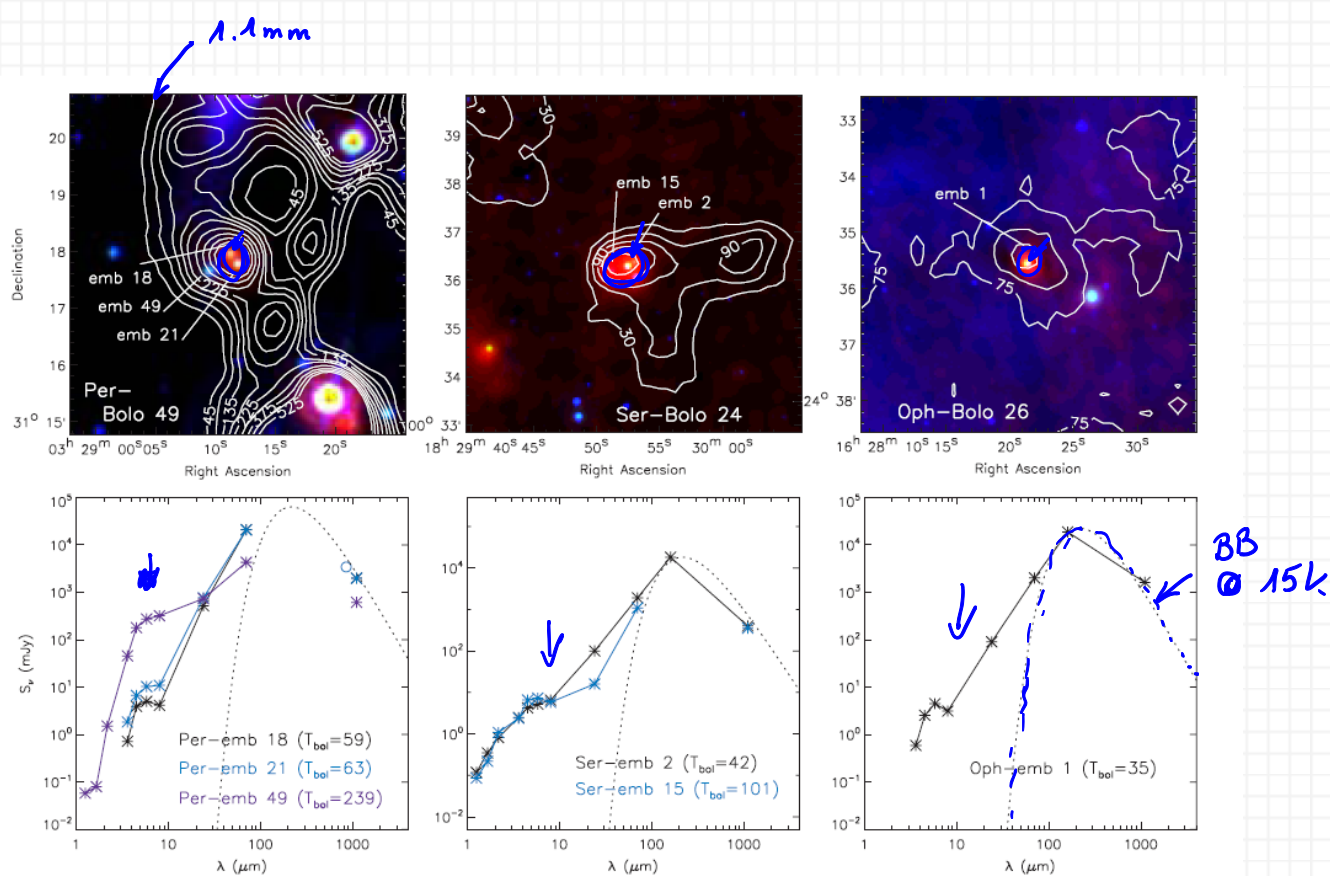


Figure 1. Three-color *Spitzer* images $8\ \mu\text{m}$ (blue), $24\ \mu\text{m}$ (green), and $70\ \mu\text{m}$ (red) of selected embedded protostar candidates in Perseus, Serpens, and Ophiuchus, with Bolocam $1.1\ \text{mm}$ contours. The Bolocam ID of the centered core and embedded protostar IDs from Tables 2–4 given, and contour intervals for the $1.1\ \text{mm}$ emission are $3, 6, \dots, 15, 20, 25, \dots, \sigma$. SEDs of the candidates are plotted in the lower panels. SEDs include 2MASS, IRAC, and MIPS photometry from the c2d database and $1.1\ \text{mm}$ fluxes (asterisks). Published $350\ \mu\text{m}$ and $850\ \mu\text{m}$ points (open circles) are also shown when available. A modified blackbody spectrum ($T = 15\ \text{K}$, $\beta = 1$) is overlaid for reference.

$1.1\ \text{mm}$ (Bolocam) contours of cool dust overlaid on Spitzer hot dust/PAH emission, (Enoch et al. 2009)

emission seen in IR because envelope is optically thick in optical.

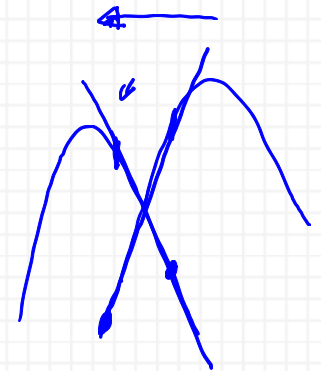
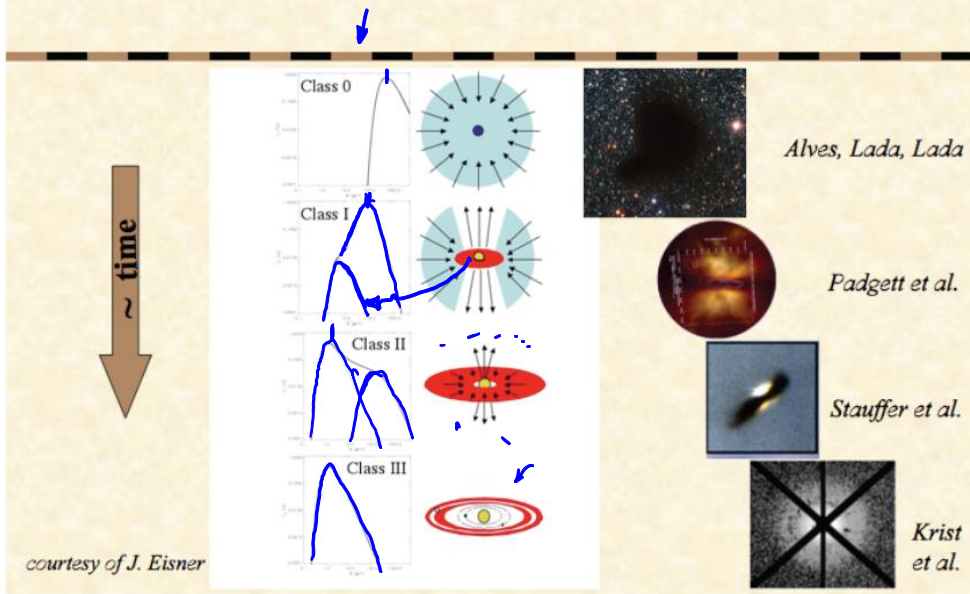
→ radiation absorbed by dust and reemitted in IR

Once we have a detection in IR → classification by SED shape
(SED: spectral energy distribution)

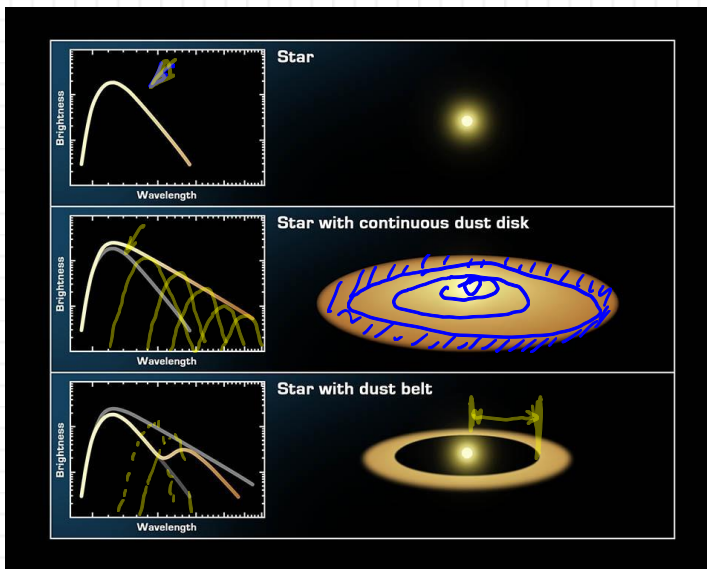
The more mass in the envelope around the protostar the more opaque it is and the further into the IR the radiation will have to shift before it can escape!

Objects with a SED peak further in the IR have a more massive envelope, therefore its accretion did not proceed for a long time → younger object

Evolution of Circumstellar Dust/Gas



Formally, classification based on flux measurements by the IRAS satellite:



1 Courtesy NASA/JPC-Caltech

$$\alpha_{IR} = \frac{d \log(\lambda F_{\lambda})}{d \log \lambda}$$

infrared spectral index

in practice: 2 IRAS points (2.2 μm and 10-25 μm)

$\alpha > 0$ peak at longer wavelength (IR)

$\alpha < 0$ peak at shorter wavelength (opt)

$\alpha > 0$ in [2 μm , 25 μm] \rightarrow class I source

Alternative classification: bolometric temperature (Myers & Lada 93)

T_{bol} of a spectrum F_{ν} is the temperature of a black body having the same mean frequency $\bar{\nu}$

$$T_{bol} = \frac{\zeta(4)}{4 \zeta(5)} \frac{h \bar{\nu}}{k} = 1.25 \times 10^{-11} \bar{\nu} \text{ K Hz}^{-1}$$

$\zeta(n)$: Riemann Zeta function of argument n

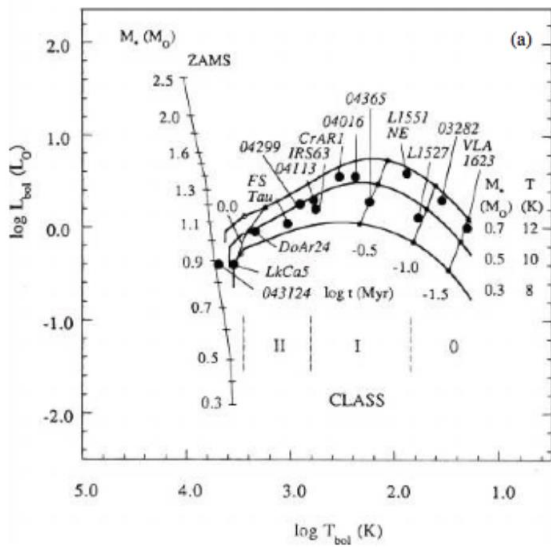
$\bar{\nu}$: mean frequency, i.e. ratio of 1st and 0th frequency moment of the spectrum

$$\bar{\nu} = \frac{I_1}{I_0}$$

and

$$I_m = \int_0^\infty \nu^m F_\nu d\nu$$

$$\frac{\int \nu F_\nu d\nu}{\int F_\nu d\nu}$$



class 0 $T_{bol} < 70 K$

class I $T_{bol} = 70 - 650 K$

class II $T_{bol} = 650 - 2880 K$

class III $T_{bol} > 2880 K$

Figure 2 (Andre et al. 2000)

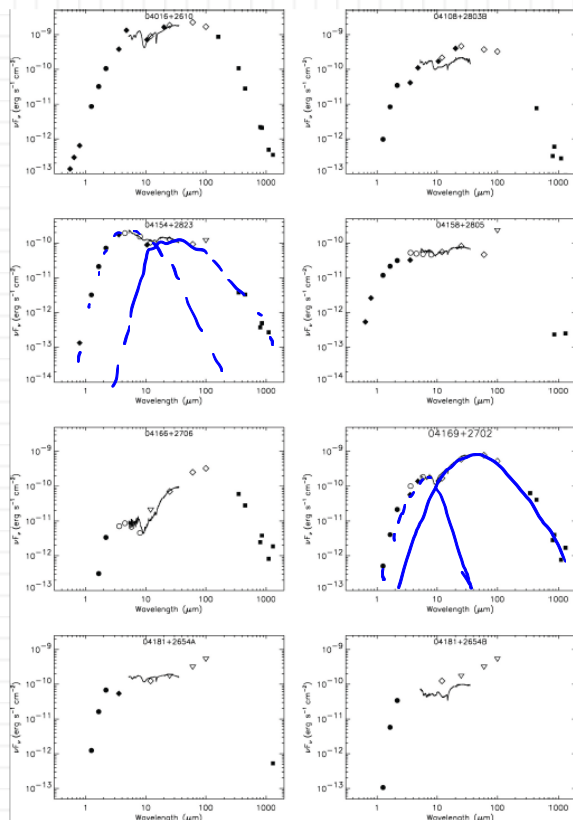
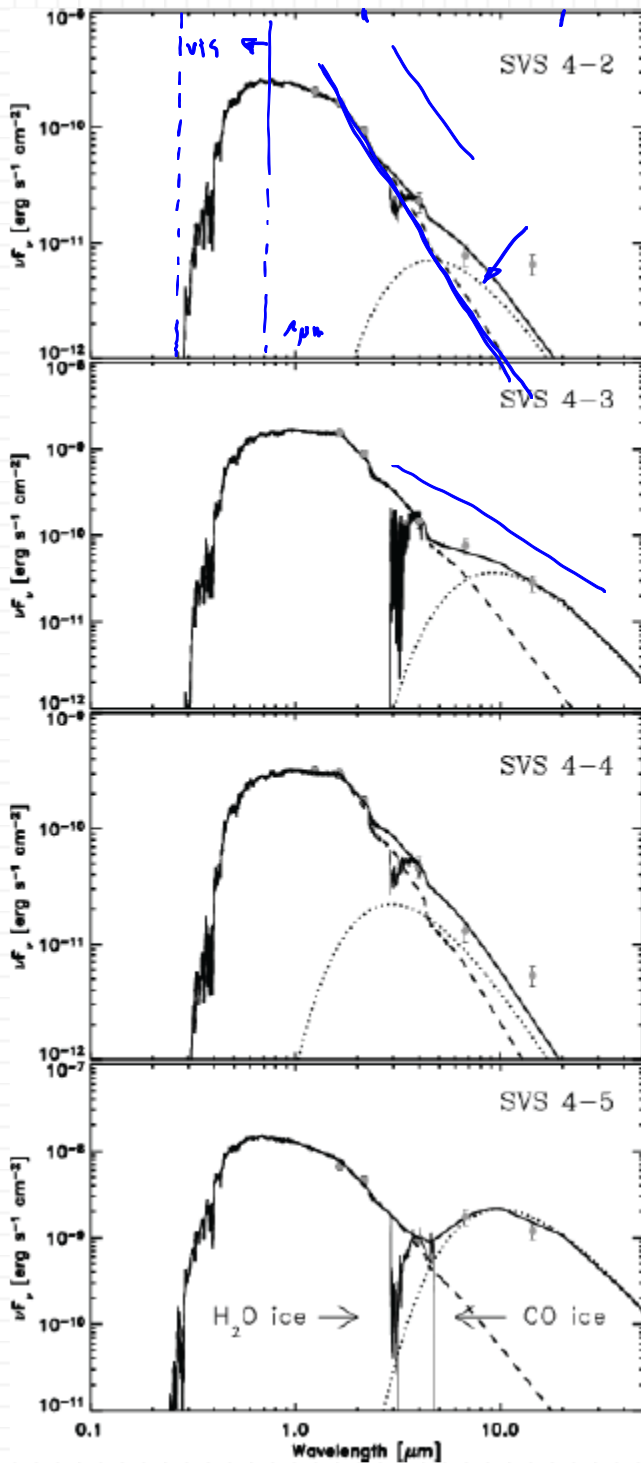


Figure 3: SEDs of class I protostars in Taurus (Furlan et al. 2008)

2.1.3 CLASS II sources

After sufficient accretion → stellar photosphere becomes visible

⇒ SED = SED_{star} + SED_{disk} (IR excess)



aka T Tauri star

(obs. definition of T Tauri stars is slightly different though)

$$-1.5 < \alpha_{IR} < 0$$

$\alpha_{IR} = -1.5$: no disk

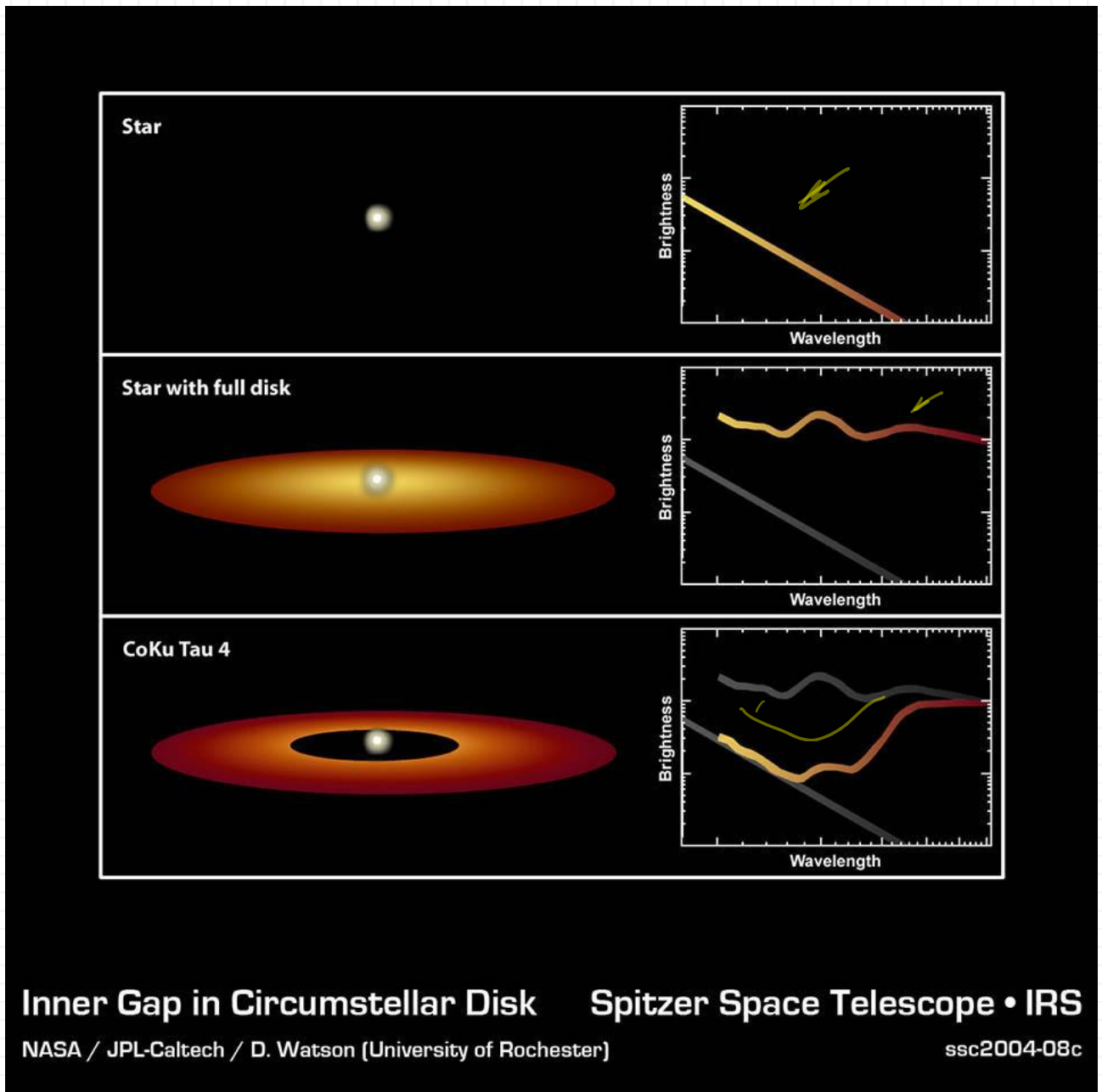
planet formation must occur during this stage because soon the accretion disk will be gone

Figure 4 SEDs of Class II sources in Serpens (Pontoppidan et al. 2004)

2.1.4 Class III sources

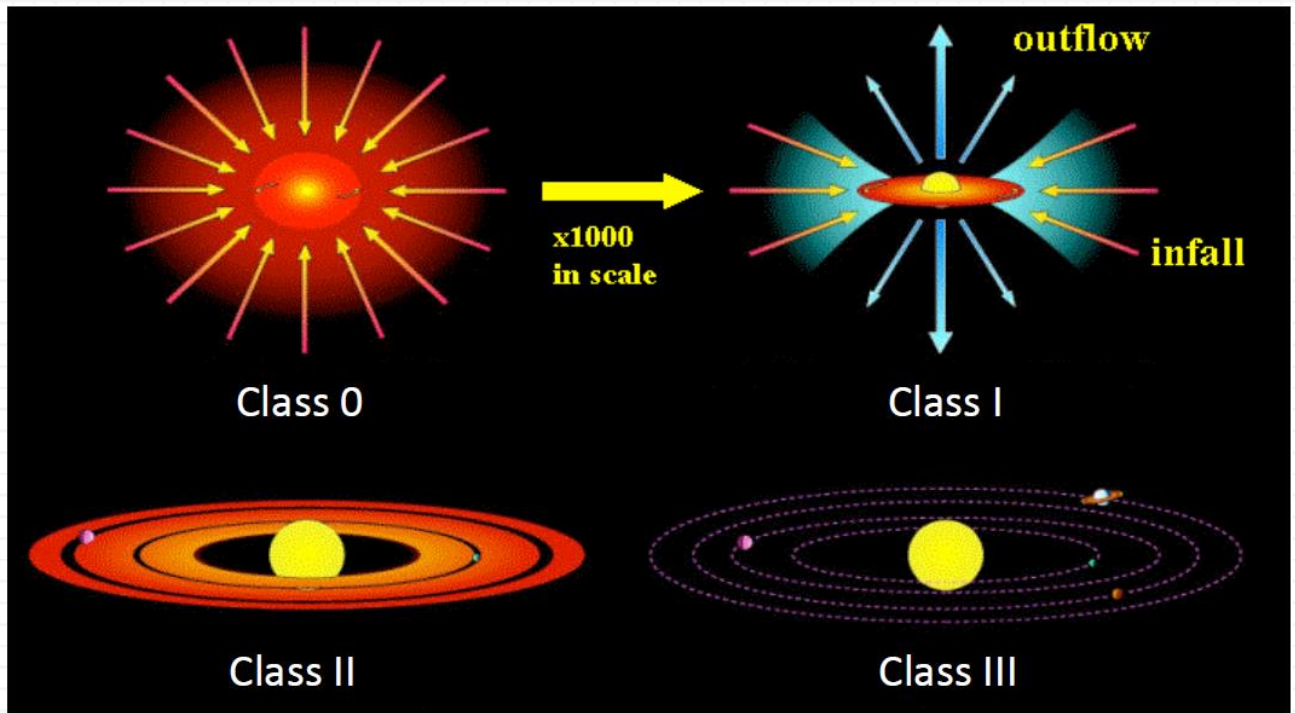
$$\alpha_{IR} < -1.5$$

SED: bare photospheric SED, any IR excess weak, i.e. cool & far from star



- disk dissipates
- not yet MS star *Energy due to grav. contraction*
 - puffed up => larger radius
 - $L > L_{MS}$
 - $T < T_{MS}$
 - high level of magnetic activity

- strong X-ray emission
- Lithium absorption lines
 - Li quickly destroyed in nuclear synthesis
 - Li not yet used up, i.e. star is still very young



Lada 1987

2.2 STATISTICS OF RESOLVED STELLAR POPULATIONS

2.2.1 Multiple Stars

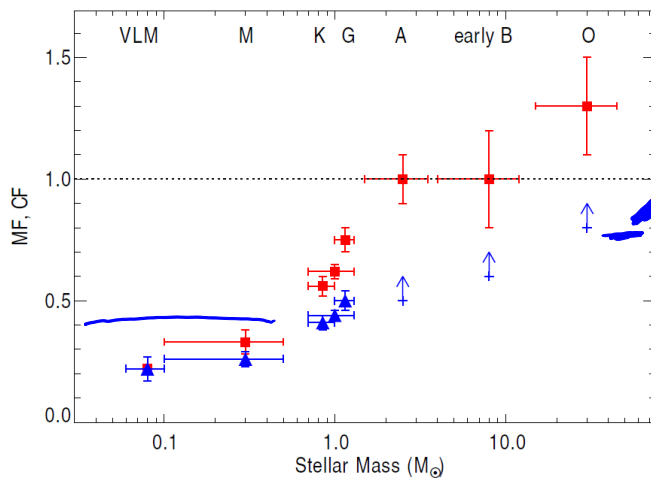


Figure 1:

Dependency of CF (red squares) and MF (blue triangles) with primary mass for MS stars and field VLM objects. The horizontal errorbars represent the approximate mass range for each population. For B and O stars, only companions down to $q \approx 0.1$ are included. The frequencies plotted here are the best-estimate numbers from Sections 3.1–3.5, also reported in Table 1.

Figure 5(Duchene & Kraus 2013)

MF: frequency of multiple systems $0 \leq MF \leq 1$

CF: companion frequency (average number of companion per target, which can exceed 100%)

The difference between these two quantities: frequency of high-order multiple systems.

significant fraction of stars in multiple systems

multiplicity: function of stellar mass

most stars are singles, most massive stars are multiples

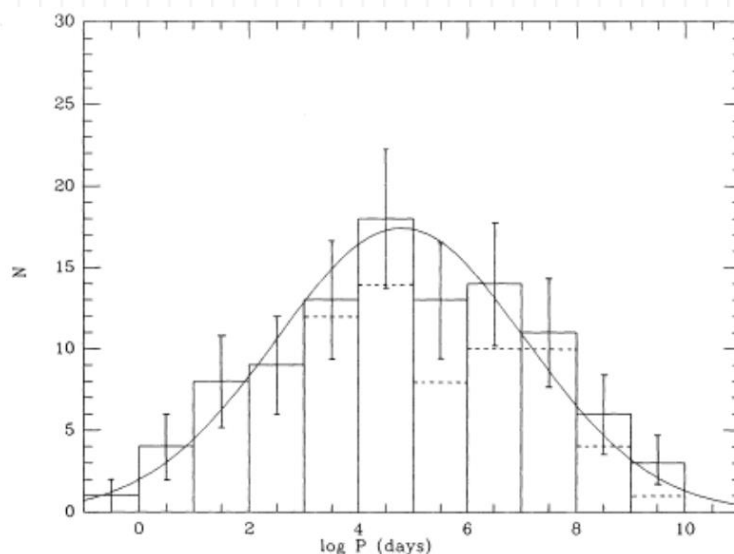


Figure 6 Binary period distribution for solar neighborhood G dwarfs (Duquennoy & Mayor 1991)

broad distribution of binary period (hrs to Myr)

WHAT IS THE ORIGIN OF THE BINARY FRACTION AND THE BINARY PERIOD DISTRIBUTION?

2.2.2 The IMF

initial mass function

in clustered SF: count young stars as function of their mass

- initial mass function (IMF)
(see: [Annu. Rev. Astron. Astrophys. 2010.48:339-389.](#))

Problem: we measure luminosities not masses

Determine the IMF:

- stars in the solar neighborhood
 - many, i.e. good statistics
 - no remaining gas & dust, i.e. no reddening
 - stars are on the MS (takes ~ 10 Myr)
- stars in young clusters
 - massive stars only found in young clusters
 - brown dwarfs fade with age, i.e. difficult to find outside of young clusters
 - stars are chemically homogeneous

no massive stars

Problems: correct for unresolved binaries

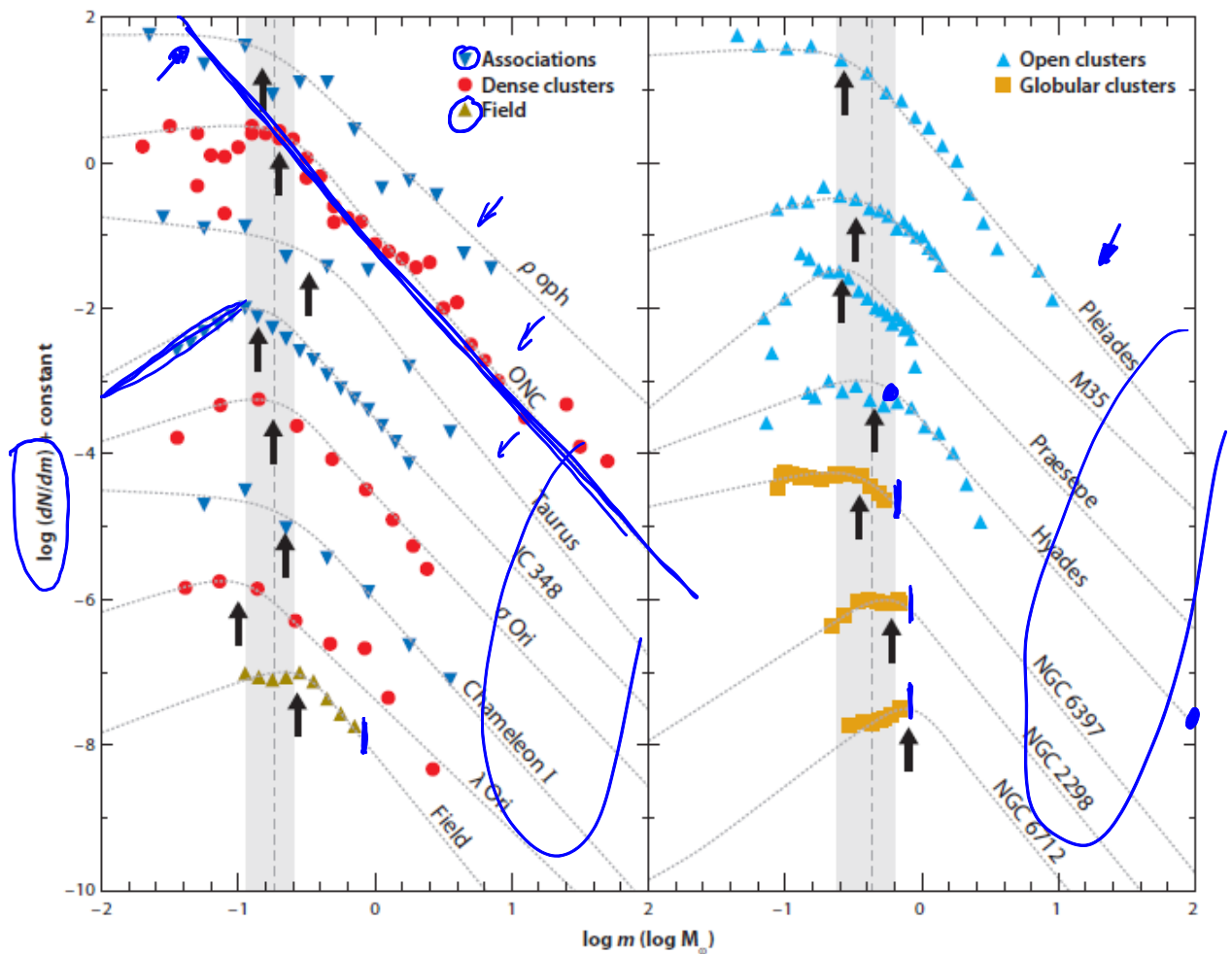


Figure 3

The derived present-day mass function of a sample of young star-forming regions (Section 2.3), open clusters spanning a large age range (Section 2.2), and old globular clusters (Section 4.2.1) from the compilation of G. de Marchi, F. Parsecse, and S. Portegies Zwart (submitted). Additionally, we show the inferred field star initial mass function (IMF) (Section 2.1). The gray dashed lines represent "tapered power-law" fits to the data (Equation 6). The black arrows show the characteristic mass of each fit (m_p), the dotted line indicates the mean characteristic mass of the clusters in each panel, and the shaded region shows the standard deviation of the characteristic masses in that panel (the field star IMF is not included in the calculation of the mean/standard deviation). The observations are consistent with a single underlying IMF, although the scatter at and below the stellar/substellar boundary clearly calls for further study. The shift of the globular clusters characteristic mass to higher masses is expected from considerations of dynamical evolution.

Figure 7 (Bastian et al. 2010)

- break peak at $\sim 0.2 M_{\odot}$
- fall off at higher masses \sim power law
- fall off at lower masses, much more uncertain

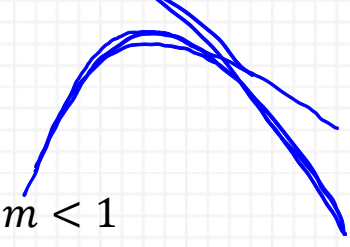
Different functional forms:

Salpeter (1955):

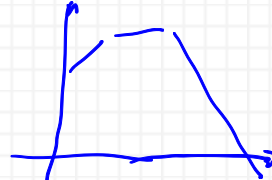
$$\frac{dn}{d \log m} \propto m^{-\Gamma} \quad \text{with} \quad \Gamma = 1.35$$

m : mass of a star, n : number of stars in the logarithmic mass range $\log m + d \log m$. Salpeter slope: $\Gamma \sim 1.35$.

Chabrier (2003):

$$\frac{dn}{d \log m} \propto \begin{cases} \exp\left(-\frac{(\log m - \log 0.22)^2}{2 \times 0.57^2}\right), & m < 1 \\ \exp\left(-\frac{(\log 0.22)^2}{2 \times 0.57^2}\right) m^{-1.35}, & m \geq 1 \end{cases}$$


Kroupa (2001):

$$\frac{dn}{d \log m} \propto \begin{cases} \left(\frac{m}{m_0}\right)^{-\alpha_0}, & m_0 < m < m_1 \\ \left(\frac{m_1}{m_0}\right)^{-\alpha_0} \left(\frac{m}{m_1}\right)^{-\alpha_1}, & m_1 < m < m_2 \\ \left[\prod_{i=1}^n \left(\frac{m_i}{m_{i-1}}\right)^{-\alpha_i}\right] \left(\frac{m}{m_n}\right)^{-\alpha_n}, & m_{n-1} < m < m_n \end{cases}$$


with

$$\begin{aligned} \alpha_0 &= -0.7 \pm 0.7, & 0.01 < \frac{m}{M_\odot} < 0.08 \\ \alpha_1 &= 0.3 \pm 0.5, & 0.08 < \frac{m}{M_\odot} < 0.5 \\ \alpha_2 &= 1.3 \pm 0.3, & 0.5 < \frac{m}{M_\odot} < 1 \\ \alpha_3 &= 1.3 \pm 0.7, & 1 < \frac{m}{M_\odot} \end{aligned}$$

2.3 UNRESOLVED STELLAR POPULATIONS AND EXTRAGALACTIC SF

What, if individual stars can't be resolved. How to study SF then? Instead of star counts, IMF, etc. we study the star formation rate (SFR)

2.3.1 Star formation rate indicators

2.3.1.1 General Theory

Stars born with IMF $\frac{dn}{dm}$, the mean stellar mass for this IMF is \bar{m} . After time t (after the star is born) it has the luminosity $L(m, t)$.

- 1) Consider a population of stars born at $t = 0$. At time t , the luminosity of the stars is:

$$L(t) = N_{\star} \int_0^{\infty} dm L(m, t) \frac{dn}{dm}$$

N_{\star} : total number of stars

normalized IMF: $\int \left(\frac{dn}{dm} \right) dm = 1$

- 2) Consider a galaxy forming stars at a rate $\dot{M}_{\star}(t)$
 $\dot{N}_{\star}(t) = \dot{M}_{\star}(t) / \bar{m}$

Then, the luminosity is

$$L = \int_0^{\infty} dt \left| \frac{\dot{M}_{\star}(t)}{\bar{m}} \int_0^{\infty} dm L(m, t) \frac{dn}{dm} \right.$$

$\dot{M}_{\star}(t)$: star formation history, usually unknown

We assume: $\dot{M}_{\star}(t) = \dot{M}_{\star} = \text{const}$ and $L(m, t > t_{\max}) = 0$

$$L = \frac{\dot{M}_{\star}}{\bar{m}} \int_0^{\infty} dm \frac{dn}{dm} \int_0^{\infty} dt L(m, t) = \frac{\dot{M}_{\star}}{\bar{m}} \int_0^{\infty} dm \frac{dn}{dm} \langle Lt_{\text{life}} \rangle_m$$

$\langle Lt_{\text{life}} \rangle_m$: total amount of energy radiated by a star of mass m over its lifetime (calculate from stellar structure and evolution theory)

If we know the IMF $\frac{dn}{dm}$ and $\langle Lt_{\text{life}} \rangle_m$ and measure L we can derive the star formation rate.

BALANCE BETWEEN NEW STARS FORMING AND OLD STARS DYING -> NUMBER OF STARS PRESENT DEPENDS ON SFR, I.E. MEASUREMENT OF STELLAR LIGHT MEASURES THE SFR!

How good is the assumption of $\dot{M}_{\star}(t) = \dot{M}_{\star} = \text{const}$?

E.g. in an entire galaxy, \dot{M}_* is probably const on timescales much shorter than the dynamical time ~ 200 Myr in the Milky Way. If we observe the luminosity at a wavelength where the light is coming mostly from stars with $t_{life} < t_{dyn}$, then $L(m, t) \rightarrow 0$ at $t < t_{dyn}$, then a constant SFR is a reasonable assumption.

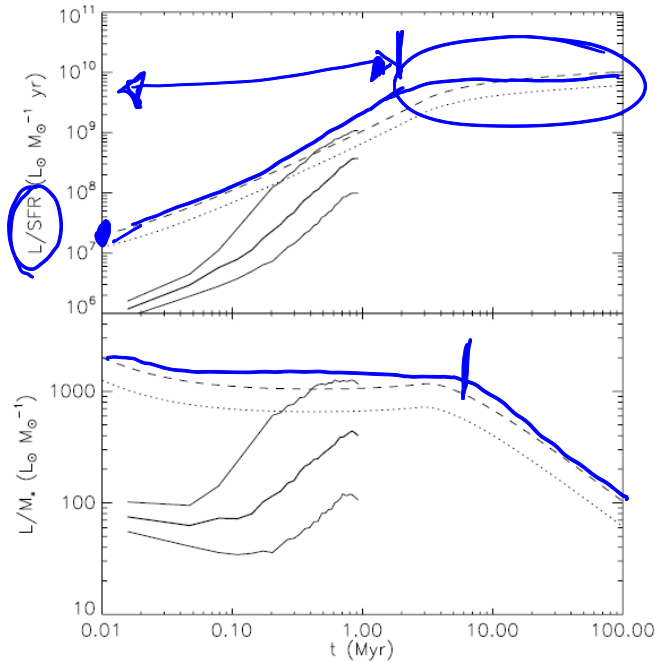


FIG. 1.—Ratio of luminosity to star formation rate (upper panel) and of luminosity to stellar mass (lower panel) vs. time for a stellar population forming at a constant rate. We show the following computations: using Starburst99 version 5.0 (Leitherer et al. 1999; Vázquez & Leitherer 2005) with the default parameters (dashed lines); using Starburst99 with an IMF that has a slope of -2.35 from $0.1 M_\odot$ to $120 M_\odot$ (dotted lines); and the median (thick solid lines) and 1σ upper and lower limits (thin solid lines) for 400 cluster simulations computed with the model of Tan & McKee (2002). Further details are given in § 2.1.3.

Figure 8 (Krumholz & Tan 2007)

CONSTRAINT:

SFR needs to be constant on timescales long compared to lifetimes of stars that generate the luminosity we measure

E.g. (left) after initiating SF it takes ~ 4 Myr to reach equilibrium, i.e. const. L/SFR ratio.

\Rightarrow measure luminosities dominated by very massive stars (short t_{life})

- techniques to detect massive stars

$$T > 15000 \text{ K}$$

2.3.1.2 Recombination Lines

Hydrogen recombination lines:

- can be used from ground
- most common technique



quiescent galaxies (E4, Sa)

actively star forming galaxies (Sc, Sm/Im)

Magellanic clouds

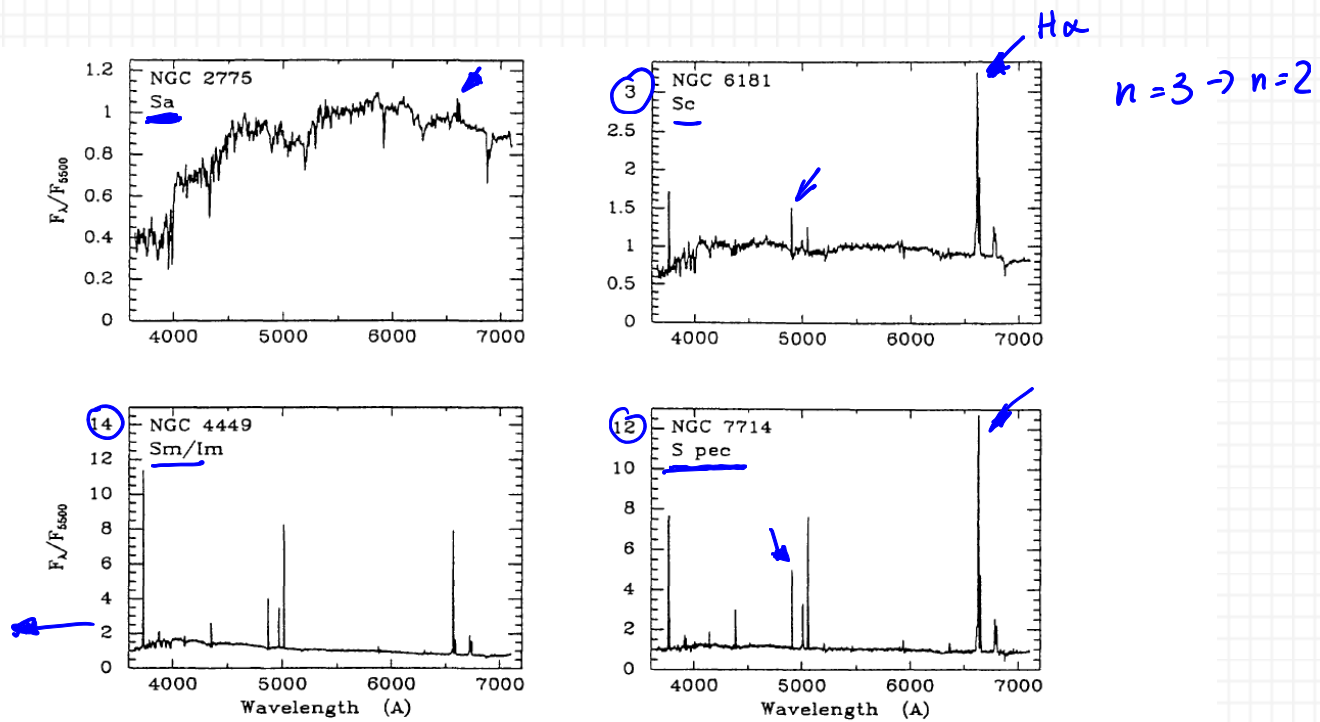


Figure 2. Integrated spectra of 4 nearby spiral and irregular galaxies, from the sample of Kennicutt (1992b).

Abbildung 9 (Kennicutt 1998)

Most prominent lines:

$H\alpha$ at 6563 Å (3→2 electronic transition)

$H\beta$ at 4861 Å (4→2 electronic transition)

In the IR, the most common lines are:

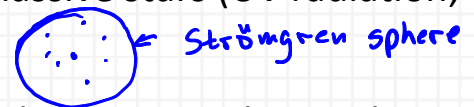
Paschen α and β at 1.87 and 1.28 μm (4→3 and 5→3)

Bracket α and γ at 4.05 and 2.17 μm (5→4 and 7→4)

$H\text{II}$: singly ionized H

HI : neutral H
 HeIII : He^{++}

Origin: from HII regions, produced by young massive stars (UV radiation, $M > 10-20$)



Ionized atoms sometimes recombine to excited states → radiative decay to ground level.

To convert the observed line luminosity to a SFR:

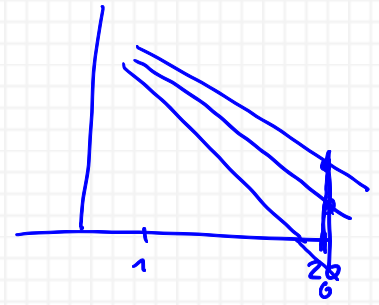
- 1) quantum statistics: yield of photons in various lines per recombination
- 2) total recomb. rate = total ionization rate
 → total rate of emission for line per ionizing photon
- 3) compute $\langle L_{\text{line}} \rangle_m$ from stellar models

← number of ionizing photon emitted by star

4) compute $\int_0^\infty dm \frac{dn}{dm} \langle L_{life} \rangle_m$ to get $L = \frac{\dot{M}_*}{\bar{m}} \times const$

ISM dominates uncertainty:

- luminosity dominated by massive stars
- numbers dominated by low mass stars



E.g. stars with $M > 15M_\odot$ provide 99% of the light and below 1% of the mass. Slight changes in the slope change L significantly.

Optical recombination lines are absorbed by dust -> correction of luminosities

2.3.1.3 Radio free-free

HII regions also emit free-free radiation in the radio \rightarrow bremsstrahlung of free electrons scattering off ions

flux from HII regions $S \propto n_e n_i$, recombination rate $R \propto n_e n_{H^+}$ therefore $S \propto$ rate of ionizing photons injected into the HII region

e.g.: from Rabidoux et al. (20124)

$$\left(\frac{L_T}{\text{W Hz}^{-1}} \right) \sim 5.5 \times 10^{20} \left(\frac{\nu}{\text{GHz}} \right)^{-0.1} \left(\frac{\text{SFR}_T(M \geq 5M_\odot)}{M_\odot \text{yr}^{-1}} \right)$$

L_T : thermal luminosity (free-free), $\nu = 33 \text{ GHz}$

Advantage: radio emission is not absorbed by dust (only technique possible in the MW!)

Disadvantage: free-free emission rather weak, additional radio emission (non-thermal) e.g. synchrotron emission needs to be separated which can

only be done when we resolve individual HII regions => only possible in MW and nearby galaxies

2.3.1.4 Infrared

In dustiest galaxies recombination lines become too absorbed.

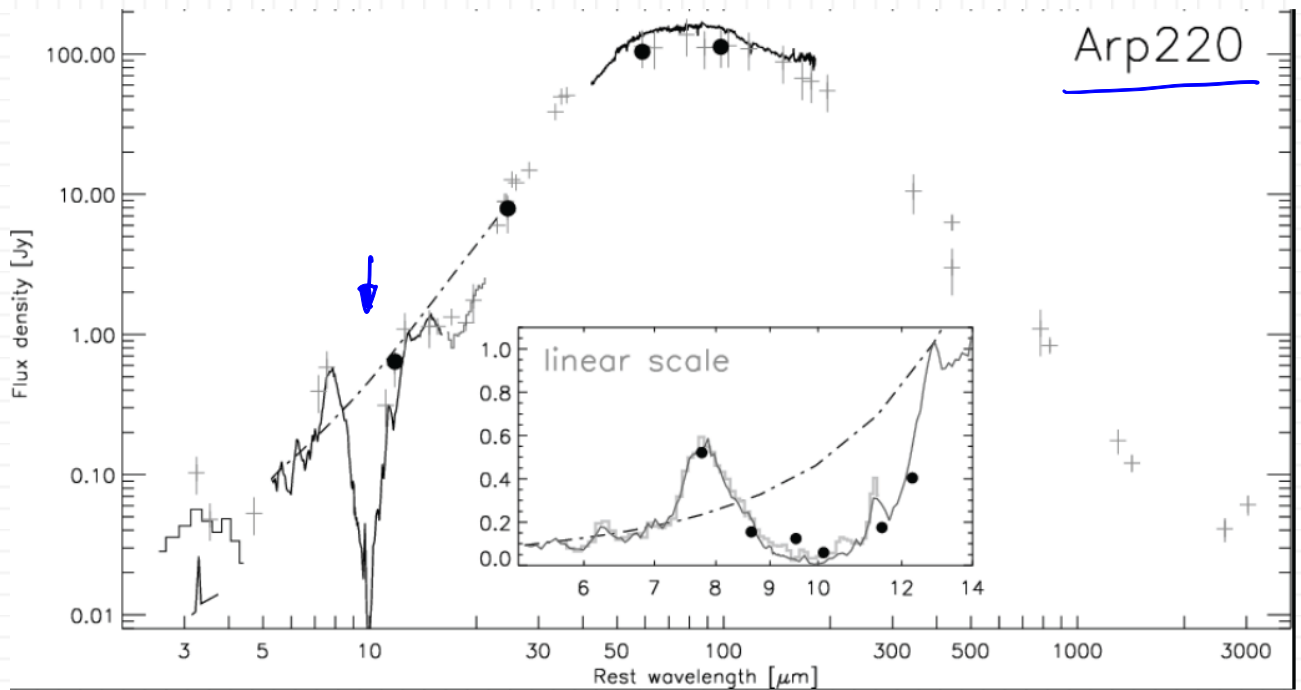
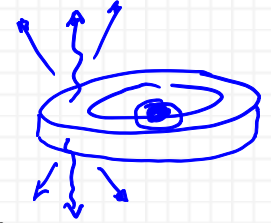


Figure 10 IR SED of Arp 220

If sufficient dust => all photons of massive stars absorbed by dust and reemitted in the IR, e.g. in starbursts

- ⇒ total IR output of galaxy measures total bolometric power of the stars in that galaxy.
- ⇒ in galaxies with high SFR this bolometric power is dominated by young stars => n

$$L(m, t) \propto L_{bol}$$



Problems:

- we miss all opt. UV photons that escape the galaxy without absorption by dust
- in case of low SFR, L_{bol} might not be dominated by young stars, so we overestimate the SFR *active galactic nucleus*
- L_{bol} can be contaminated by AGN contribution

2.3.1.5 UV

broadband UV flux at wavelength $> 912 \text{ \AA}$ but shorter than the peak emission of older stars: $\lambda = 1250 - 2500 \text{ \AA}$ (cannot ionize H)

Observable from ground if redshifted

Observable from space: GALEX (1300-1800 \AA FUV, and 1800-2800 \AA NUV)

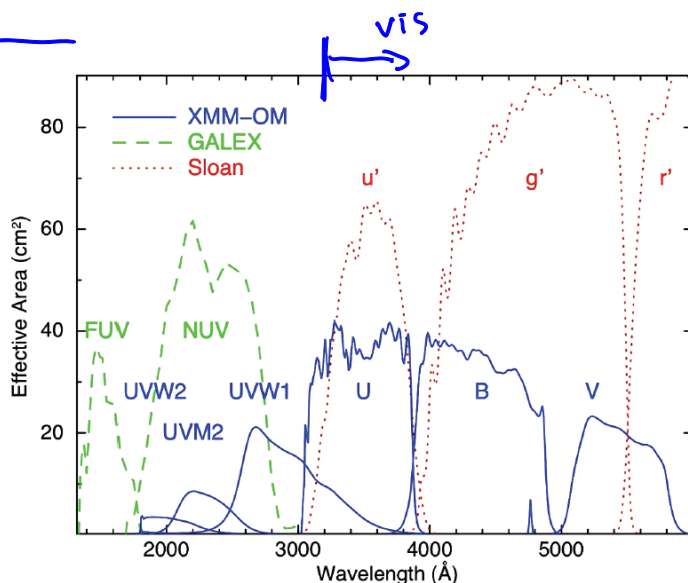


Figure 11 GALEX bandpass compared to other instruments

emission dominated by

$$M \sim 5M_{\odot}$$

with lifetimes of $\sim 50 \text{ Myr}$

L_{FUV} measures SFR integrated over this time

Problems:

- long timescales -> SFR needs to be constant a long time
- in smaller regions stars may move away, etc.
- also suffers from dust extinction

2.3.1.6 Combined estimators

Best way to determine SFR is by combining multi-wavelength measurements

2.3.2 The Kennicutt Law (1998)

empirical relation between gas in galaxies and their SFR

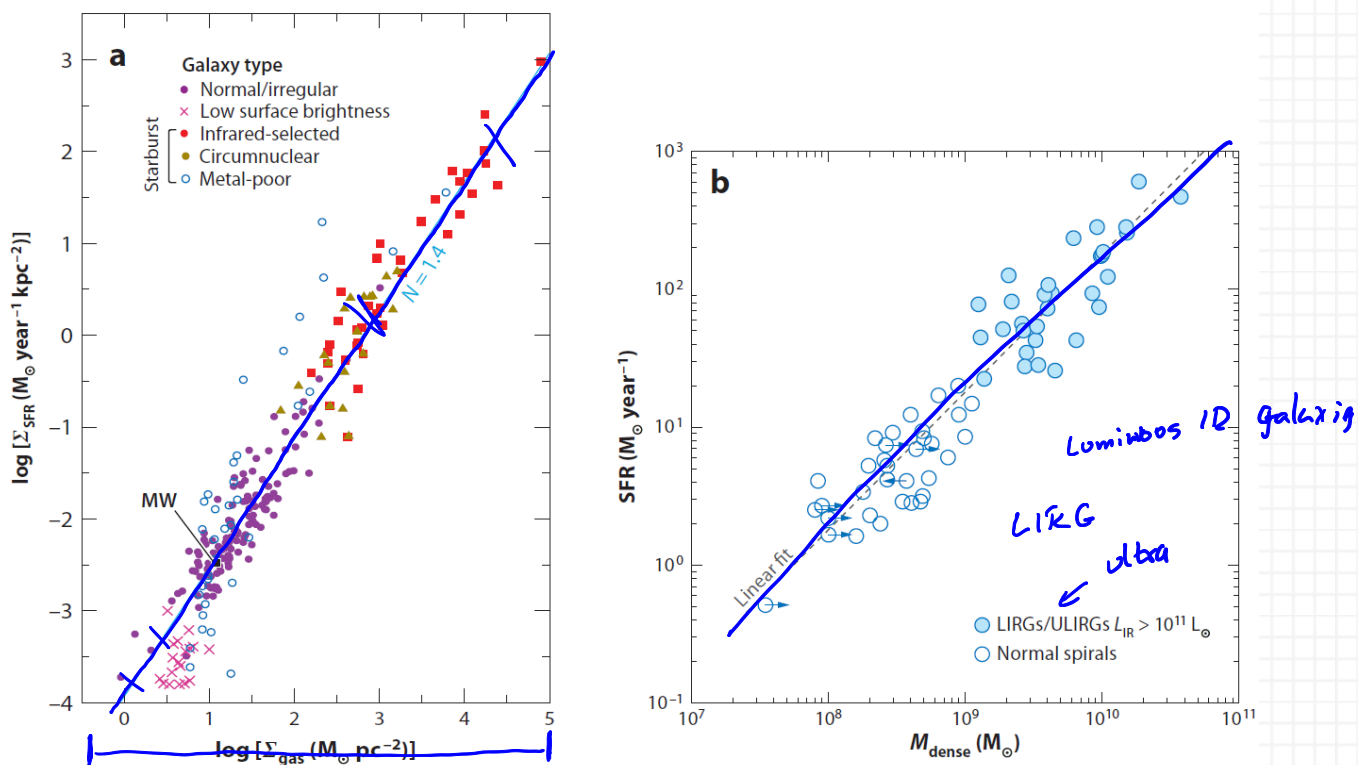


Figure 12 Kennicutt & Evans 2012

SFR per unit area of the galaxy disk against gas mass per unit disk area

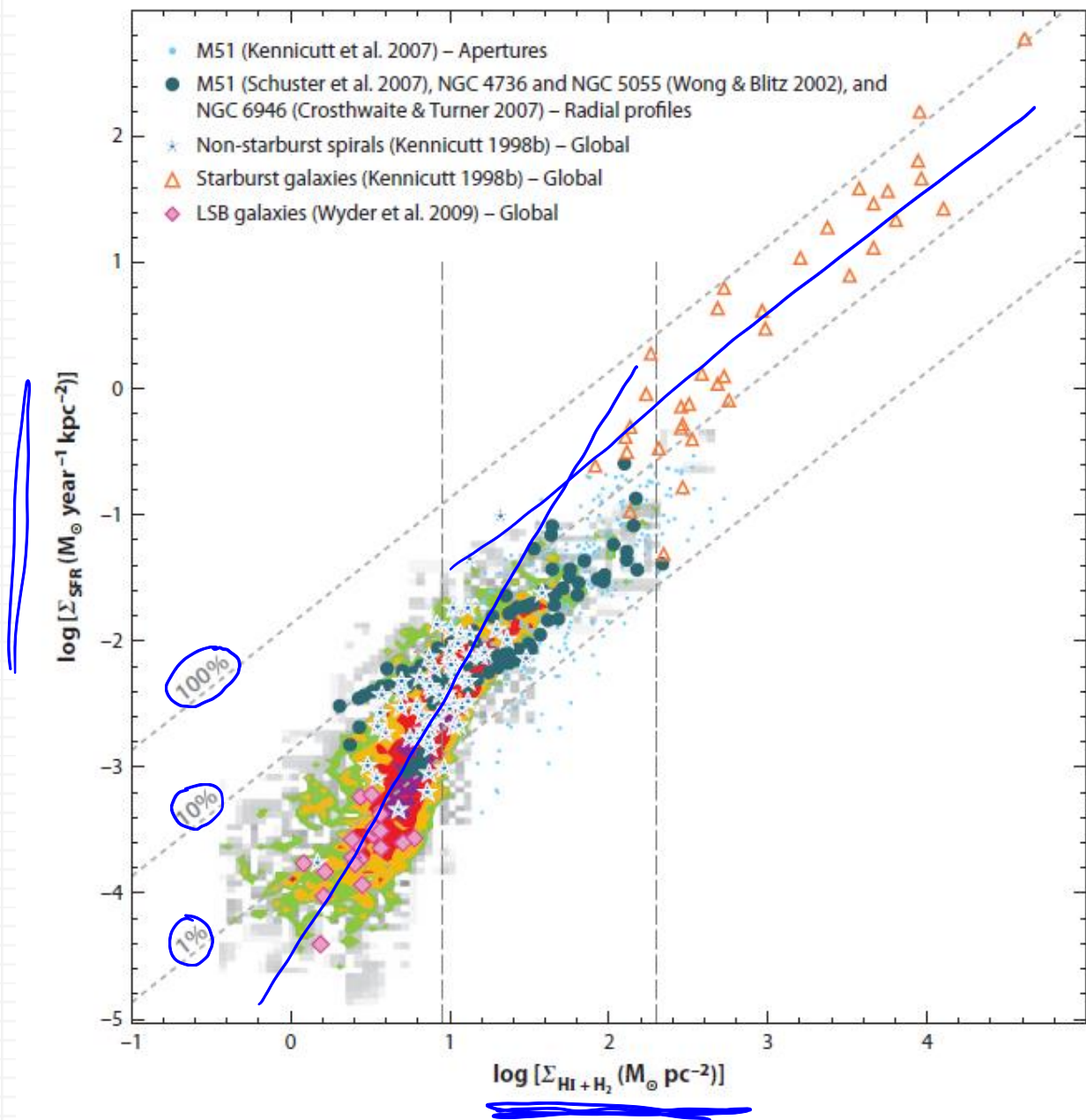
$$\Sigma_{SFR} [M_{\odot} \text{ yr}^{-1} \text{ kpc}^{-2}] = 2.5 \times 10^{-4} (\Sigma_{gas} [M_{\odot} \text{ pc}^{-2}])^{1.4}$$

Also: good correlation involving the angular velocity of rotation Ω at the edge of the star-forming region of the disk

$$\Sigma_{SFR} = 0.017 \Sigma_{gas} \Omega$$

(averages over whole galaxies)

more complete sample shows deviations of simple power law (see Bigiel et al. 2008)



origin unclear.

WHAT IS THE ORIGIN OF THE KENNICUTT LAW?

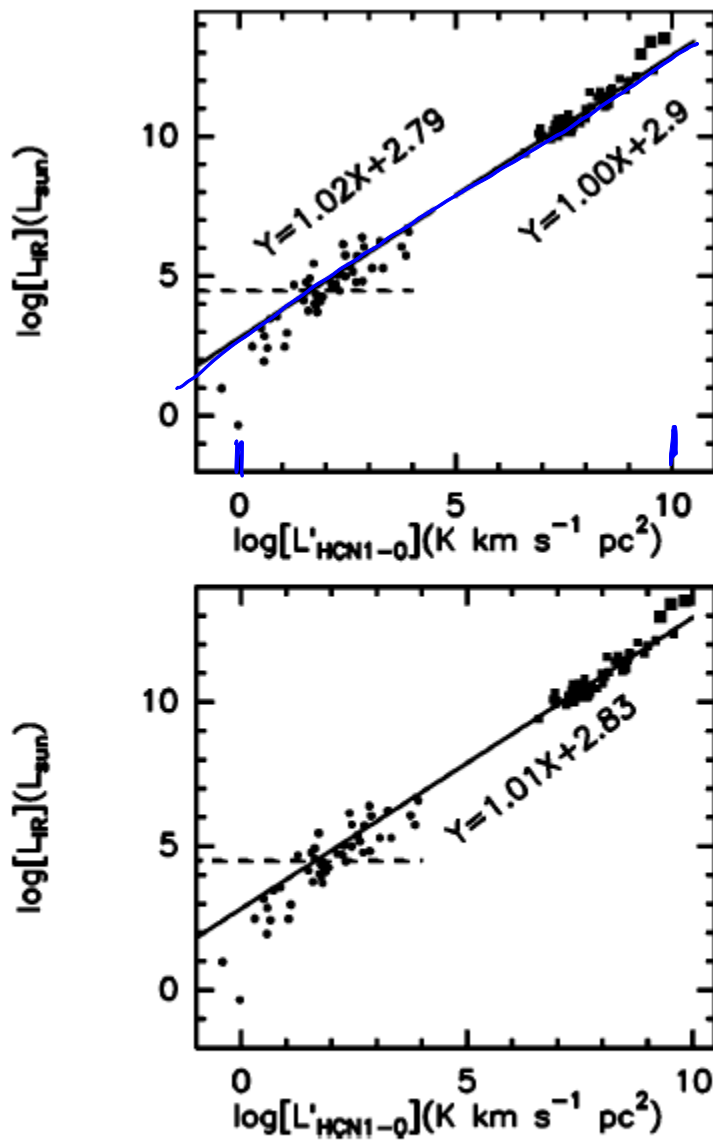


FIG. 1.— $\log L_{\text{IR}} - \log L'_{\text{HCN1-0}}$ correlation for Galactic and extragalactic sources. *Top*: Linear least-squares fit for Galactic cores (with $L_{\text{IR}} > 10^{4.5} L_{\odot}$; symbols above the dashed line) and for galaxies, separately. *Bottom*: Overall fit for both parts. The three isolated filled squares are high- z HCN 1-0 points from Solomon et al. (2003), Vanden Bout et al. (2004), and Carilli et al. (2005); they are not included in the fit because the sources are QSOs and the contribution from the active galactic nucleus to L_{IR} is not yet clear.

Figure 13 Wu et al. 2005

IR-HCN correlation

IR \propto SFR

HCN \propto gas mass above
critical density ($\sim 10^5 \text{ cm}^{-3}$)

tight correlation over 10
orders of magnitude!